Degradation Process of Lead Chromate in Paintings by Vincent van Gogh Studied by Means of Spectromicroscopic Methods. 3. Synthesis, Characterization, and Detection of Different Cry...

ARTICLE *in* ANALYTICAL CHEMISTRY · JANUARY 2013

Impact Factor: 5.64 · DOI: 10.1021/ac302158b

analytical chemistry

Article

pubs.acs.org/ac

Degradation Process of Lead Chromate in Paintings by Vincent van Gogh Studied by Means of Spectromicroscopic Methods. 3. Synthesis, Characterization, and Detection of Different Crystal Forms of the Chrome Yellow Pigment

Letizia Monico,[†,‡] Koen Janssens,[*,‡] Costanza Miliani,[§] Brunetto Giovanni Brunetti,[†,§] Manuela Vagnini,[∥] Frederik Vanmeert,[‡] Gerald Falkenberg,[⊥] Artem Abakumov,[@] Yinggang Lu,[@] He Tian,[@] Johan Verbeeck,[@] Marie Radepont,[‡,#] Marine Cotte,[#,▽] Ella Hendriks,[○] Muriel Geldof,[◆] Luuk van der Loeff,[¶] Johanna Salvant,[□] and Michel Menu[□]

[†]Centre SMAArt and Dipartimento di Chimica, Università degli Studi di Perugia, via Elce di Sotto 8, I-06123 Perugia, Italy

[‡]Department of Chemistry, University of Antwerp, Groenenborgerlaan 171, B-2020 Antwerp, Belgium

[§]Istituto CNR di Scienze e Tecnologie Molecolari (CNR-ISTM), c/o Dipartimento di Chimica, Università degli Studi di Perugia, via Elce di Sotto 8, I-06123 Perugia, Italy

[∥]Associazione Laboratorio di Diagnostica per i Beni Culturali, piazza Campello 2, I-06049 Spoleto (Perugia), Italy

[⊥]Hamburger Synchrotronstrahlungslabor HASYLAB at Deutsches Elektronensynchrotron DESY, Notkestr. 85, D-22603 Hamburg, Germany

[@]Department of Physics (EMAT), University of Antwerp, Groenenborgerlaan 171, B-2020 Antwerp, Belgium

[#]Laboratoire d'Archéologie Moléculaire et Structurale, CNRS UMR8220, 3, rue Galilée, F-94200 Ivry-Sur-Seine, France

[▽]European Synchrotron Radiation Facility (ESRF), 6, rue Jules Horowitz, F-38000 Grenoble, France

[○]Van Gogh Museum, Paulus Potterstraat 7, 1070 AJ Amsterdam, The Netherlands

[◆]Movable Heritage Knowledge Sector, The Netherlands Cultural Heritage Agency (RCE), Hobbemastraat 22, 1071 ZC Amsterdam, The Netherlands

[¶]Conservation Department, Kröller-Müller Museum, Houtkampweg 6, NL-6731AW Otterlo, The Netherlands

[□]Centre de Recherche et de Restauration des Musées de France (C2RMF), Palais du Louvre, Porte des Lions, 14 Quai François Mitterrand, F-75001 Paris, France

S *Supporting Information*

ABSTRACT: The painter, Vincent van Gogh, and some of his contemporaries frequently made use of the pigment chrome yellow that is known to show a tendency toward darkening. This pigment may correspond to various chemical compounds such as $PbCrO_4$ and $PbCr_{1-x}S_xO_4$, that may each be present in various crystallographic forms with different tendencies toward degradation. Investigations by X-ray diffraction (XRD), mid-Fourier Transform infrared (FTIR), and Raman instruments (benchtop and portable) and synchrotron radiation-based micro-XRD and X-ray absorption near edge structure spectroscopy performed on oil-paint models, prepared with in-house synthesized $PbCrO_4$ and $PbCr_{1-x}S_xO_4$, permitted us to characterize the spectroscopic features of the various forms. On the basis of these results, an extended study has been carried out on historic paint tubes and on embedded paint microsamples taken from yellow-orange/pale yellow areas of 12 Van Gogh paintings, demonstrating that Van Gogh effectively made use of different chrome yellow types. This conclusion was also confirmed by in situ mid-FTIR investigations on Van Gogh's *Portrait of Gauguin* (Van Gogh Museum, Amsterdam).

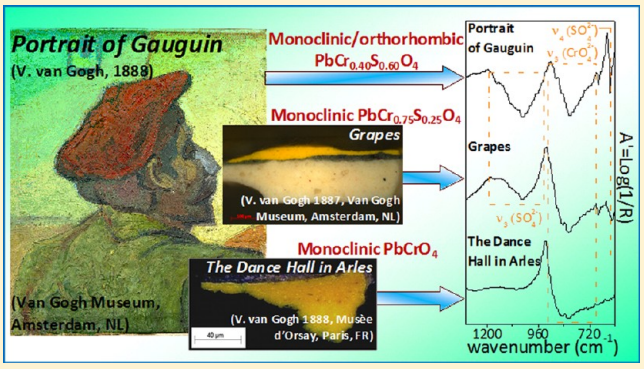

Historical and more recent documentations report that chrome yellow pigments were widely used by Van Gogh[1] and his contemporaries.[2−4] They are characterized by different

Received: July 14, 2012
Accepted: October 10, 2012
Published: October 10, 2012

Table 1. Composition of In-House Synthesized/Commercial Lead Chromate-Based Powders and Historic Chrome Yellow Paint A and Corresponding XRD Results

		bench-top powder XRD[a]		
sample[b]	starting CrO_4^{2-}:SO_4^{2-} molar ratio/description	phases	space group	mass fraction (%)
S^*_{1mono}	1:0	$PbCrO_4$	monoclinic $P2_1/n$	98.82(5)
		$PbCrO_4$	orthorhombic *Pnma*	1.18(6)
S^*_{3A}	0.9:0.1	$PbCr_{0.89}S_{0.11}O_4$	monoclinic $P2_1/n$	100
S^*_{3B}	0.75:0.25	$PbCr_{0.76}S_{0.24}O_4$	monoclinic $P2_1/n$	100
S^*_{3C}[c]	0.5:0.5	$PbCr_{0.54}S_{0.46}O_4$	monoclinic $P2_1/n$	60.0(2)
		$PbCr_{0.09}S_{0.91}O_4$	orthorhombic *Pnma*	31.1(1)
		$PbCrO_4$	orthorhombic *Pnma*	9.10(8)
S^*_{3D}[c]	0.25:0.75	$PbCr_{0.6}S_{0.4}O_4$	monoclinic $P2_1/n$	11.5(3)
		$PbCr_{0.1}S_{0.9}O_4$	orthorhombic *Pnma*	74.7(3)
		$PbCrO_4$	orthorhombic *Pnma*	13.8(2)
D^*_1	commercial $PbCr_{1-x}S_xO_4$ (CIBA and BASF)	$PbCr_{0.52}S_{0.48}O_4$	monoclinic $P2_1/n$	75.0(1)
		$PbSO_4$	orthorhombic *Pnma*	25.0(1)
A[c]	historic oil paint tube belonging to the Flemish Fauvist Rik Wouters (1882−1913)	$PbCr_{0.8}S_{0.2}O_4$	orthorhombic *Pnma*	41.0(1)
		$PbCr_{0.1}S_{0.9}O_4$	orthorhombic *Pnma*	58.0(1)
		$PbCr_{0.6}S_{0.4}O_4$	monoclinic $P2_1/n$	1.0 (1.0)

[a]Data obtained via Rietveld analysis. For cell parameters see Table S-1 of the Supporting Information. [b]The XRD pattern of S^*_{1ortho} (Figure S-1 of the Supporting Information) resembles that reported in literature.[13,15] [c]Sulfur and chromium abundances were calculated as a weighted average for the mass fraction of orthorhombic and monoclinic phases. The chemical composition for S_{3C} and A was estimated as $PbCr_{0.4}S_{0.6}O_4$; for S_{3D} this was $PbCr_{0.2}S_{0.8}O_4$.

compositions [$PbCrO_4$, $PbCr_{1-x}S_xO_4$, $(1-x)PbCrO_4{\cdot}xPbO$] and crystallographic forms and have been extensively studied recently because of their limited stability (darkening) under the influence of light and other environmental factors.[3,4]

Chrome yellows available to artists today are known as Primrose Chrome ($PbCr_{1-x}S_xO_4$, $0.45 \le x \le 0.55$), Lemon Chrome ($PbCr_{1-x}S_xO_4$, $0.2 \le x \le 0.4$) and Middle Chrome (mainly pure $PbCrO_4$). The former two varieties show pale, greenish-yellow shades, while the latter has a reddish-yellow hue.[5,6] Van Gogh, in several paint orders of 1888−1890,[7] already mentioned the use of chrome yellow types 1, 2, and 3, corresponding to "lemon", "yellow", and "orange" shades.

From the crystallographic point of view, $PbCrO_4$ and $PbSO_4$ show monoclinic[8,9] and orthorhombic[10] structures, respectively. In $PbCr_{1-x}S_xO_4$ solid solutions, when x exceeds 0.4, a change from a monoclinic to an orthorhombic structure is observed.[11−13] Under specific experimental conditions, the less stable orthorhombic $PbCrO_4$ may be synthesized.[14,15]

Our previous investigations on both artificially aged model samples of commercial chrome yellow pigments[3] and two paint microsamples taken from paintings by Van Gogh[4] demonstrated that the chrome yellow alteration is caused by the reduction of original Cr(VI) to Cr(III), as highlighted by the spatial correlation between the brown alteration and the local Cr(III) concentration.

Moreover, we found that only the sulfate-rich historic paint model featured a significant darkening after photochemical aging, while in original samples the alteration products [Cr(III) species] was encountered especially in areas rich in S, Ba, and/or Al/Si.

On the basis of these results,[3,4] the available literature about the UV aging[9] and synthesis[16] of chrome yellow pigments based on 19th century recipes, and the analysis of chromate materials taken from historic paintings and paint tubes,[17] this work is aimed to extend and deepen the insight in the way sulfates may influence the stability of this class of pigments.

For this purpose, we have synthesized and characterized different crystal forms of $PbCrO_4$ and $PbCr_{1-x}S_xO_4$ ($0.1 \le x \le 0.75$) by employing X-ray diffraction (XRD), mid-Fourier Transform infrared (mid-FTIR), Raman, synchrotron radiation-based micro XRD (SR μ-XRD), and S K-edge micro-X-ray absorption near edge structure spectroscopy (μ-XANES). Complementary information was collected by scanning transmission electron microscopy (STEM) equipped with energy dispersive X-ray (EDX) spectrometry. An extended study was carried out on pigments from historic paint tubes and on microsamples from paintings by Van Gogh and his contemporaries. The results demonstrate that it is possible to distinguish among the various orthorhombic and monoclinic forms of $PbCrO_4$ or $PbCr_{1-x}S_xO_4$, and that Van Gogh and his contemporaries effectively made use of these different chrome yellow pigments.

In the companion paper (part 4 of the series),[18] by the artificially aging of the aforementioned chrome yellow-based model paints, we demonstrate that different forms of chrome yellows show a strong different tendency toward darkening. To be able to distinguish among these different varieties is therefore very relevant, since it may open up the possibility to investigate whether there is an effective correlation between the chrome yellow composition/crystalline structure and its preservation state in original paintings.

EXPERIMENTAL SECTION

Synthesis of $PbCrO_4$ and $PbCr_{1-x}S_xO_4$ and Preparation of Paint Models. The synthesis of monoclinic $PbCrO_4$ powder (S^*_{1mono}, where * denotes pure inorganic powder without an organic binder added) and several $PbCr_{1-x}S_xO_4$ solid solutions with increasing x values, (S^*_{3A}, S^*_{3B}, S^*_{3C}, S^*_{3D}) was performed following Crane et al.,[13] while the preparation of orthorhombic $PbCrO_4$ (S^*_{1ortho}) was accomplished according to Xiang et al.[15] (see the Supporting Information for further details about the synthesis). Table 1 shows the properties of the synthesized lead chromate-based compounds.

Paint models (S_1−S_{3D}) were prepared by mixing the powders with linseed oil in a 4:1 weight ratio and applying the mixture on polycarbonate microscopy slides. Employing the same procedure, two further paints were prepared: the first, hereby indicated as D_1, by mixing oil and a commercial pigment (CIBA and BASF), while the other, D_2, was made of oil, $PbCrO_4$, and $PbSO_4$

dx.doi.org/10.1021/ac302158b | Anal. Chem. 2013, 85, 851−859

Table 2. List of the Original Embedded Paint Microsamples and Historic Chrome Yellow Pigments Investigated

Origin of paint sample	Sample number/ name	Chrome yellow composition		Techniques for detecting the chrome yellow type	PANTONE Hue
		$PbCrO_4$	$PbCr_{1-x}S_xO_4$[a]		
Historic oil paint tube belonging to the Dr. Gachet collection (ca. 1890) (Berthaut, Paris) (M'O)	DG_1	monoclinic	-	XRD,[b] Raman, FTIR	(109C)
	DG_2[c]	-	monoclinic	XRD,[b] Raman, FTIR	(130C)
Rik Wouters's oil paint tube (1882-1913) (Mommen & Cie, Brussels) (Royal Museum of Fine Arts, Antwerp)	A		orthorhombic	XRD, Raman. FTIR	(3945C)
Historic oil paint tube (end 19th century) (Elsens, Brussels) (Royal Academy of Fine Arts, Antwerp)	B_1		monoclinic	XRD,[b] Raman, FTIR	(108C)
	B_2[c]		monoclinic	XRD,[b] Raman, FTIR	(130C)
Bank of the Seine, 1887 (VGM)	F293/3		monoclinic	XRD,[d] Raman	(109C)
Grapes, 1887 (VGM)	F603/3		monoclinic	XRD,[d] Raman, FTIR	(108C)
Sunflowers gone to seed, 1887 (VGM)	F377/2	monoclinic		Raman	(109C)
Self-portrait with straw hat, 1887 (VGM)	F469/2[e]	orthorhombic		XRD,[d] Raman	(387C)
Quinces, lemons, pears and grapes, 1887 (VGM)	F383/4[e]	difference not detectable		Raman	(3945C)
Field with flowers near Arles, 1888 (VGM)	F409/1	monoclinic		XRD,[f] Raman, FTIR	(109C)
The bedroom, 1888 (VGM)	F482/7[c]	monoclinic		XRD,[d] Raman, FTIR	(1375C)
	F482/8	monoclinic		XRD,[d] Raman, FTIR	(3945C)
The Dance Hall in Arles ("Ball in Arles"), 1888 (M'O)	10872	monoclinic		XRD,[f] Raman, FTIR	(109C)
Falling leaves (Les Alyscamps), 1888 (KMM)	224/1		monoclinic and possibly orthorhombic	XRD,[d] Raman, FTIR	(3945C)
Portrait of Gauguin, 1888 (VGM)	X448_2		monoclinic and possibly orthorhombic	XRD,[d] Raman	(3945C)
Sunflowers, 1889 (VGM)	F458/3		monoclinic and possibly orthorhombic	XRD,[d] Raman	(393C)
	F458/1	monoclinic	monoclinic	XRD,[d] Raman, FTIR	(109C)/ (3945C)
Tree roots, 1890 (VGM)	F816/3		monoclinic and possibly orthorhombic	XRD,[d] Raman, FTIR	(108C)
Be mysterious, P. Gauguin, 1890 (M'O)	2751		monoclinic and possibly orthorhombic	XRD,[f] Raman, FITR	(3945C)
Van Gogh palette, 1890 (M'O)	10455		monoclinic	XRD,[f] Raman, FTIR	(116C)/ (393C)
Cézanne palette (M'O)	10426		monoclinic and possibly orthorhombic	XRD,[f] Raman, FTIR	(108C)

[a]Monoclinic: $PbCr_{1-x}S_xO_4$ is more similar to the reference S_{3B}. Monoclinic and possible orthorhombic: $PbCr_{1-x}S_xO_4$ is more similar to the reference S_{3C} (see text for details). [b]XRD performed by employing only the portable instrumentation. An indirect semiquantitative estimation of the S amount was also performed by SEM-EDX (Figure S-4 of the Supporting Information). [c]Mixture of chrome yellow and orange [phoenicochroite − (1−x)-$PbCrO_4$•xPbO]. [d]SR μ-XRD performed at DESY/PETRA III facility (beamline P06) (Hamburg, Germany). [e]Mixture of chrome and zinc yellow. [f]SR μ-XRD performed at DESY/DORIS III facility (beamline L) (Hamburg, Germany).

powders (both Aldrich), the latter two mixed in a 1:2 molar ratio.

Original Samples. *Historic Oil Paint Tubes.* In addition to the already investigated historic chrome yellow paints A, B_1, and B_2 belonging to late 19th century artists,[3] two other paint samples (denoted below as DG_1 and DG_2), supplied by the Musée d'Orsay (M'O, Paris, France), were taken from two oil-paint tubes originally belonging to the Dr. Paul Gachet collection, assumed to have been used by Van Gogh.[19] Some of their properties are reported in Table 2 and in the Supporting Information.

Embedded Micropaint Samples. Table 2 also shows some properties and results obtained from the investigation of fifteen micropaint samples from chromium-based yellow areas of twelve paintings by Van Gogh, one by Gauguin, and two other samples from the palettes of Cézanne and Van Gogh; these materials were

dx.doi.org/10.1021/ac302158b | Anal. Chem. 2013, 85, 851−859

supplied by the Kröller-Müller Museum (KMM, Otterlo, The Netherlands), the M'O, and the Van Gogh Museum (VGM, Amsterdam, The Netherlands). For sake of brevity, in this paper only the results acquired from the microsamples of the following five Van Gogh paintings [*Grapes* (1887, VGM, F603/3), *Field with flowers near Arles* (1888, VGM, F409/1), *Falling leaves (Les Alyscamps)* (1888, KMM, 224/1), *The Dance Hall in Arles ("Ball in Arles")* (1888, M'O, 10872), *Tree roots* (1890, VGM, F816/3)] are discussed in detail. Results collected from a sample taken from Van Gogh's palette that he used in Auvers-sur-Oise (1890, M'O, 10455)[19] are also presented.

Noninvasive in Situ Investigations. In addition to studies on paint samples, reflection mid-FTIR measurements[20] were directly performed on Van Gogh's *Portrait of Gauguin* (VGM, F546 s257v/1962, painted in December 1888).

Analytical Methods. The following methods were used to investigate both paint models and original samples: benchtop, portable and SR μ-XRD, high-angle annular dark field (HAADF)/STEM-EDX; S K-edge SR μ-XANES; benchtop and portable mid-FTIR; benchtop and portable Raman. Details about the instruments and the experimental conditions are described in the Supporting Information.

RESULTS AND DISCUSSION

Characterization of Paint Models. *XRD and HAADF/STEM-EDX.* A combination of XRD and HAADF/STEM-EDX mapping were used to determine the morphology, the S and Cr local distributions, and the phase composition of in-house synthesized and commercial $PbCr_{1-x}S_xO_4$.

Diffractograms [Figure 1A (top panel) and Figure S-1 of the Supporting Information] of powders recorded by the benchtop equipment (black) are similar to those collected from the corresponding paint models at the PETRA-III SR-facility (blue). Rietveld refinement (Table 1) indicates that powders S^*_{1mono}, S^*_{3A}, and S^*_{3B} are composed of a single monoclinic phase (a minor amount of orthorhombic $PbCrO_4$ is present in S^*_{1mono}). As in the work by Crane et al.[13], the lattice parameters (Table S-1 of the Supporting Information) of each $PbCr_{1-x}S_xO_4$ phase decrease with increasing S content. This is observable on the recorded patterns (Figure 1A, bottom panel) by a progressive shift of the diffraction peaks toward higher Q values [see e.g., (111) and (020) peaks of the S^*_{1mono}–S^*_{3D} monoclinic phase].

While the fraction of monoclinic $PbCr_{1-x}S_xO_4$ decreases to ca. 60 wt % in S^*_{3C} and 11.5 wt % in S^*_{3D}, the orthorhombic equivalents (such as $PbCr_{0.1}S_{0.9}O_4$) become more prevalent (ca. 30 wt % in S^*_{3C} and ca. 75 wt % in S^*_{3D}). A contribution of 9–14 wt % of orthorhombic $PbCrO_4$ is also present in these samples. In powder D^*_1, although revealing an elemental composition similar to that of S^*_{3C}, monoclinic $PbCr_{1-x}S_xO_4$ is the main constituent; the presence of some orthorhombic $PbSO_4$ was also observed.

The combined use of HAADF-STEM (Figure S-2 of the Supporting Information) and STEM-EDX in the investigation of S_{3B} and S_{3D} (Figure 1B and Figure S-2C of the Supporting Information for S_{3C} results) revealed the presence of nanocrystals of two different shapes and elemental composition: Cr-rich elongated rods of variable size (ca. 200–500 nm) and S-rich globular particles (ca. 50 nm diameter). Consistent with the average XRD results (Table 1), literature data,[15] and STEM-EDX quantitative analysis (Figure 1B), the rods correspond to monoclinic phases and the globular particles to orthorhombic ones.

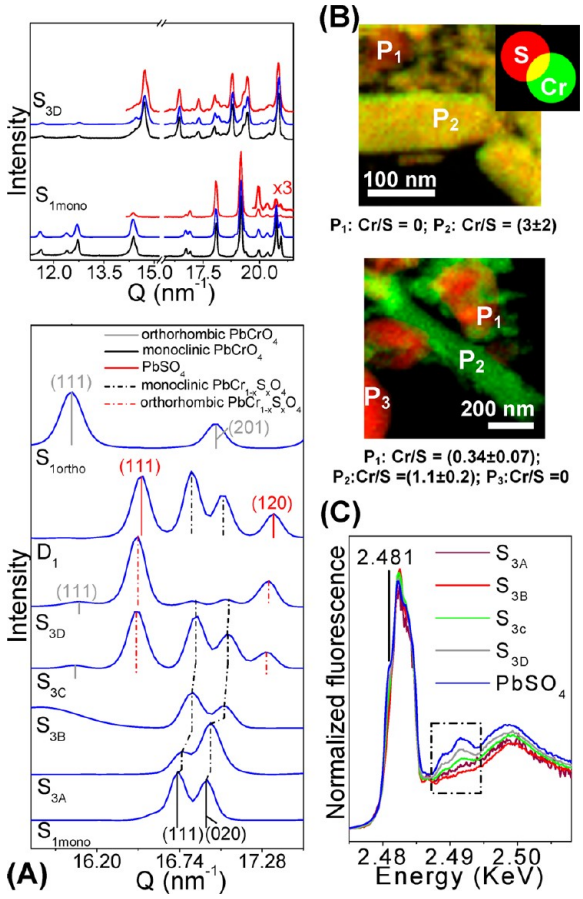

Figure 1. (A) (top) XRD patterns of S_{1mono} (monoclinic $PbCrO_4$) and S_{3D} ($PbCr_{0.2}S_8O_4$) obtained by (blue) SR (PETRA-III), (black) benchtop, and (red) portable instrumentation; (bottom) detail of SR μ-XRD patterns of $PbCrO_4$ (S_{1mono}, S_{1ortho}) and $PbCr_{1-x}S_xO_4$ (S_{3A}–S_{3D}, D_1). (B) Composite S/Cr EDX map of (top) S_{3B} and (bottom) S_{3D}. Labels "P_i" indicate the positions where quantitative analyses (in atomic %) were performed. (C) S K-edge XANES spectra of in-house synthesized $PbCr_{1-x}S_xO_4$ and commercial $PbSO_4$ paint models. [see Figures S-1 and S-2 of the Supporting Information for details on (A) and (B)].

pH measurements of 10 mL of water equilibrated with 1–2 mg of the in-house synthesized powders showed that the orthorhombic $PbCrO_4$ (S^*_{1ortho}) and the monoclinic co-precipitates (S^*_{3A}, S^*_{3B}) yielded a slightly acidic pH value (5.7 ± 0.1), while the $PbCr_{1-x}S_xO_4$ materials composed of monoclinic and orthorhombic forms (S^*_{3C}, S^*_{3D}) and $PbSO_4$ yielded a significantly lower pH (4.5 ± 0.1). The monoclinic $PbCrO_4$ (S^*_{1mono}) featured a slightly higher pH value (6.1 ± 0.1). The pH value obtained for S^*_{1ortho} is consistent with that of Crane et al.[13] and can be indirectly related to the higher solubility of the orthorhombic $PbCrO_4$ ($K_{ps} = 10^{-10.71}$, $\Delta_fG^0_{orthorhombic} = \sim 813.2$ kJ/mol) compared to that of the thermodynamically more stable monoclinic form ($K_{ps} = 10^{-12.60}$, $\Delta_fG^0_{monoclinic} = \sim 824$ kJ/mol). Similar conclusions can be drawn for the solubility of orthorhombic $PbCr_{1-x}S_xO_4$ relative to their monoclinic equivalents.

S K-edge μ-XANES. S K-edge μ-XANES spectra of $PbCr_{1-x}S_xO_4$ paint models (Figure 1C) are generally similar to that of the $PbSO_4$ reference compound, featuring a prominent peak at around 2.482 keV, specific for the sulfate species.[21,22] However, there are subtle differences when the Cr content decreases in $PbCr_{1-x}S_xO_4$: an additional pre-edge feature gradually appears on the left side of the S(VI) peak around 2.481 keV, while several

dx.doi.org/10.1021/ac302158b | *Anal. Chem.* 2013, 85, 851–859

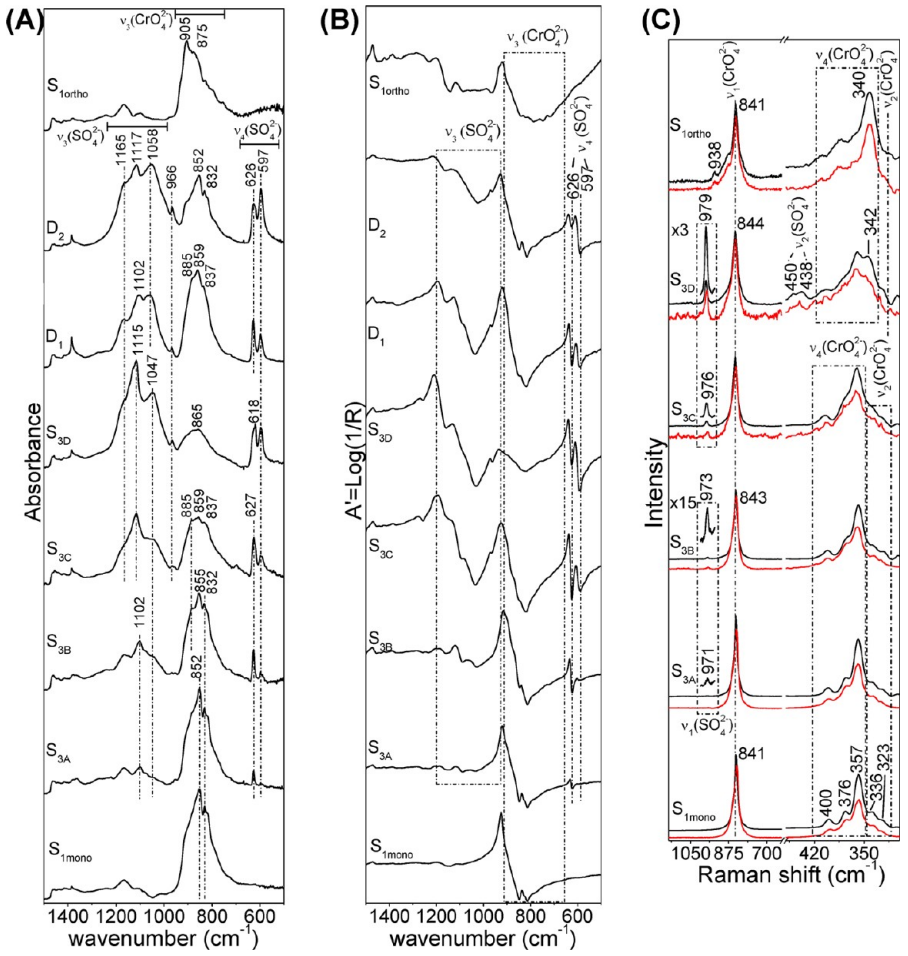

Figure 2. (A) Transmission and (B) reflection mid-FTIR spectra of paint models of $PbCrO_4$ (S_{1mono} and S_{1ortho}), $PbCr_{1-x}S_xO_4$ (S_{3A}–S_{3D}, D_1), and a mixture (D_2) of monoclinic $PbCrO_4$ and $PbSO_4$ (1:2 molar ratio). Spectra collected by benchtop and portable instruments are illustrated in (A) and (B), respectively. (C) Raman spectra of paint models S_{1mono}, S_{1ortho}, and S_{3A}–S_{3D} acquired by (black) benchtop and (red) portable devices [see Figure S-3 of the Supporting Information for details on (C)].

postedge features become more clearly defined. Figueiredo et al.[23] observed analogous features in various Fe(II) and Fe(III) sulfate minerals that were related to differences in the symmetry and nature of the S-binding site. The Figure 1C spectra are consistent with the view that in $PbSO_4$, all sulfate oxygen atoms are directly bound to Pb atoms, giving rise to a simple S(VI) XANES pattern. In the more Cr-rich co-precipitate materials the sulfate groups are more isolated, implying the disappearance of some pre- and postedge features.

Infrared Spectroscopy. Transmission Mid-FTIR. Spectra collected from paint models (Figure 2A) feature some changes when the SO_4^{2-} content increases going from S_{3A} to S_{3D}; additionally, other differences are visible in the spectra of the two polymorph forms of $PbCrO_4$ (S_{1mono}, S_{1ortho}).

In the ν_3 sulfate asymmetric stretching region, the monoclinic S_{3A} and S_{3B} show a weak signal around 1102 cm^{-1}; this band becomes stronger and moves toward higher wavenumbers (1115 cm^{-1}) in S_{3C} and S_{3D} where orthorhombic phases are present. When going from S_{3A} to S_{3D}, two additional signals around 1165 and 1047 cm^{-1} [$\nu_3(SO_4^{2-})$] become progressively visible, as well as the IR-forbidden sulfate symmetric stretching mode (ν_1 at 966 cm^{-1}).

The ν_4 sulfate asymmetric bending region is characterized by the presence of two signals at ca. 626–627 and 597 cm^{-1}. With increasing sulfate amount, a shift of the former band to 620–618 cm^{-1} is observed, while an increase of the relative intensity of the band at 597 cm^{-1} also takes place.

In the ν_3 chromate asymmetric stretching region (930–800 cm^{-1}), both a band broadening and a shift toward higher wavenumbers is detected when the amount of chromate decreases. Consistent with the XRD data (Table 1) and studies on other $MCr_{1-x}S_xO_4$ (M = Ba, Ca, Sr, Pb, and Na),[24−26] this is justified by changes in the crystalline structure.

Two bands at 852 and 832 cm^{-1} are present in the spectra of S_{1mono} and S_{3A}; their position shifts toward highest energies for S_{3B} (855 and 832 cm^{-1}) and S_{3C} (859 and 837 cm^{-1}). For these two latter samples, an additional signal around 885 cm^{-1} is visible. The spectrum of S_{3D} features a broad band around 865 cm^{-1} that shifts up to 905 cm^{-1} for S_{1ortho}. Consistent with the XRD results (Table 1), the spectral features of D_1 resemble those of S_{3C} and D_2 (the latter showing band features of both monoclinic $PbCrO_4$ and of orthorhombic $PbSO_4$).

Reflection Mid-FTIR. In order to establish whether or not it is possible to detect the differences between the various chrome yellow forms in a noninvasive manner on paintings, all paint models were examined also by reflection mid-FTIR. A comparison of Figure 2B to 2A illustrates the presence of spectral distortions. These anomalies depend on the band strength, concentration, particle size distribution, and the setup geometry.[27] The strong $\nu_3(SO_4^{2-})$ and $\nu_3(CrO_4^{2-})$ absorption bands are

dx.doi.org/10.1021/ac302158b | Anal. Chem. 2013, 85, 851–859

inverted by the reststrahlen effect, with minima at about 1030 and 822 cm^{-1}, respectively, while the weaker $\nu_4(SO_4^{2-})$ bands show a derivative shape. Consistent with the transmission mid-FTIR results, the relative intensity of the two $\nu_4(SO_4^{2-})$ signals changes, and the splitting of the $\nu_3(CrO_4^{2-})$ (860−800 cm^{-1}) disappears when the sulfate amount increases.

Raman Spectroscopy. Figure 2C shows Raman spectra of the model paints obtained by the benchtop device (black lines). Details about the mathematical treatment of spectra are reported in Figure S-3 of the Supporting Information. (Data obtained from D_1 and D_2 give results similar to those of S_{3C} and S_{1mono} and are therefore not shown).

When the sulfate amount increases, the wavenumber of the $\nu_1(CrO_4^{2-})$ stretching mode[28,29] monotonically increases from 841 cm^{-1} for $PbCrO_4$ (S_{1mono} and S_{1ortho}) to 844 cm^{-1} for S_{3C} and S_{3D} (Figures 2C and S-3A of the Supporting Information). The full width at half-maximum (fwhm) of this component also increases. These observations can be explained by the lattice compression effect and the prevention of intermolecular coupling occurring when sulfate replaces the chromate anions inside the structure.[24,25]

With increasing amount of sulfate, a progressive shift of the position toward highest energy, increase of the FWHM, and a change of the relative intensities are also seen for the components describing the chromate bending modes (400−280 cm^{-1}) (Figure S-3B of the Supporting Information). Consistent with the literature,[28,29] for S_{1mono}, the $\nu_4(CrO_4^{2-})$ modes are located at 400, 376, and 357 cm^{-1}, while those at 336 and 323 cm^{-1} are attributable to the $\nu_2(CrO_4^{2-})$ vibration. The band between 339 and 342 cm^{-1} is characteristic for the presence of orthorhombic compounds, becoming clearly visible for S_{3D} and S_{1ortho} (Figures 2C and S-3B). Similar to the chromate vibrations, the $\nu_1(SO_4^{2-})$ position shifts from 971 cm^{-1} (S_{3A}) to 980 cm^{-1} (D_2, the pure $PbSO_4$) (Figure 2C).

As done for FTIR spectroscopy, equivalent data were collected by a portable Raman spectrometer suitable for in situ analyses. Figure 2C (red lines) illustrates that, despite the lower instrumental spectral resolution, analogous systematic differences can be observed as a function of the CrO_4^{2-}:SO_4^{2-} ratio.

Identification of Different Forms of Chrome Yellow Pigments in Historic Paint-Tube Samples and Microsamples of Original Paintings. Table 2 reports a list of 22 paint samples obtained from a series of 12 paintings by Van Gogh, one Gauguin painting, the palette by Van Gogh and Cézanne, and 5 historic oil-paint tubes. In 20 cases, XRD, reflection mid-FTIR, and/or Raman spectroscopy provided appropriate information to characterize the type of chrome yellow. Among these, six showed the presence of monoclinic $PbCrO_4$, while in the others, chrome yellow was found to be present in a co-precipitated form. In this latter group, 6 of the 12 samples showed features most similar to those of S_{3B} (monoclinic $PbCr_{1-x}S_xO_4$, x = ~0.25), while the other six revealed characteristics close to those of S_{3C} (mixture of monoclinic and orthorhombic $PbCr_{1-x}S_xO_4$, $x \approx 0.50$). In one sample (F458/1), two chrome yellow forms (monoclinic $PbCrO_4$ and $PbCr_{1-x}S_xO_4$) were found, while in another one (sample A), only orthorhombic $PbCr_{1-x}S_xO_4$ was identified. For two other samples (F469/2, F383/4), neither Raman nor mid-FTIR spectroscopy allowed us to identify the exact nature of the chrome yellow present. The detection of the Raman signal at ca. 841−845 cm^{-1} (chromate stretching mode) indicates the presence of a generic lead chromate-based compound. For F469/2, an orthorhombic lead chromate-based compound was identified by SR μ-XRD, while no information was obtained for F383/4.

Consistent with the composition, the chrome yellow hue qualitatively ranges from orange-yellow for those samples containing $PbCrO_4$ and S-poor $PbCr_{1-x}S_xO_4$ compounds to the pale-yellow for those materials made of an S-rich $PbCr_{1-x}S_xO_4$. Orange and yellow-greenish shades are qualitatively given to those samples in which chrome orange (DG_2, B_2, F482/7) and zinc yellow (F469/2) were identified.

Historical Chrome Yellow Paints. In order to characterize the historic chrome yellow paints A, B_1, B_2, DG_1, and DG_2, first the sulfur amount was semiquantitatively determined via SEM-EDX (Figure S-4 of the Supporting Information), and then XRD, mid-FTIR, and Raman spectrometry were used to obtain information on the compounds present.

As Figure S-4 of the Supporting Information illustrates, in sample A ca. 62 ± 2% of the anions are sulfate. Paints B_1, B_2, and DG_2 contain less (around 33−35%), while DG_1 does not contain any measurable amount of sulfate. The high S abundance in sample A is consistent with the quantitative XRD data (Table 1), that reveal the presence of two orthorhombic phases: $PbCr_{0.8}S_{0.2}O_4$ and $PbCr_{0.1}S_{0.9}O_4$. A small amount of monoclinic $PbCr_{1-x}S_xO_4$ is also likely to be present. For this paint, Figure 3A illustrates that comparable XRD patterns were obtained by SR-based, benchtop, and, despite the lower spectral resolution, portable instrumentation.

HAADF/STEM-EDX and S K-edge XANES analyses of paint A (Figure S-5A/B of the Supporting Information) confirm the presence of the orthorhombic co-precipitate as in XRD.

Transmission mid-FTIR (Figure 3B) and Raman spectra (Figure 3C) of sample A show features that are mostly similar to the materials having an orthorhombic phase (S_{3D}/D_2, S_{1ortho}), while the spectra of the other (less S-rich) paint samples B_1, B_2, and DG_2 resemble that of monoclinic co-precipitate S_{3B}; for DG_1, the vibrational spectral features are analogous to that of monoclinic $PbCrO_4$ (cf. Table 1 and Figures 2A and 2C). These observations are confirmed by XRD (Figure 3A).

In the FTIR spectra of B_1 and B_2, the $\nu_3(CrO_4^{2-})$ and $\nu_4(SO_4^{2-})$ band shapes show differences due to the presence of $MgCO_3$, which contributes with signals around 800 and 597 cm^{-1},[3] while for DG_2 and B_2 (dark chrome yellow), additional Raman bands at 826, 376, 340, and 323 cm^{-1} are ascribable to phoenicochroite, a compound also identified by XRD.

The above-mentioned results point to the fact that the historic paint A, a material that proved itself to be very susceptible to darkening due to UVA-visible irradiation,[3] contains orthorhombic $PbCr_{1-x}S_xO_4$ phases, while the materials that proved to be significantly less prone to darkening (B_1 and B_2)[3] contain the monoclinic ones.

Embedded Paint Microsamples and Noninvasive in Situ Investigations. Investigations of the yellow areas of embedded paint microsamples F409/1, 10872, F603/3, 10455, 224/1, and F816/3 (Figure 4A) clearly demonstrate the presence of different chrome yellow forms (see also Table 2). FTIR (Figure 4B) and Raman (Figure 4C) spectra, compared to those of the reference paints S_{1mono}, S_{3B}, and S_{3C}, show that the yellow-orange paint layer of F409/1 and 10872 is composed of monoclinic $PbCrO_4$, while the lighter-yellow regions of the other ones are formed by $PbCr_{1-x}S_xO_4$. More in depth, it appears that for F603/3 and 10455, the $PbCr_{1-x}S_xO_4$ composition is close to that of the S_{3B} model in which the monoclinic structure dominates, while for F816/3 and 224/1, the spectral features resemble those of S_{3C} containing both the monoclinic and the orthorhombic form. These vibrational spectroscopic results were also confirmed

dx.doi.org/10.1021/ac302158b | *Anal. Chem.* 2013, 85, 851−859

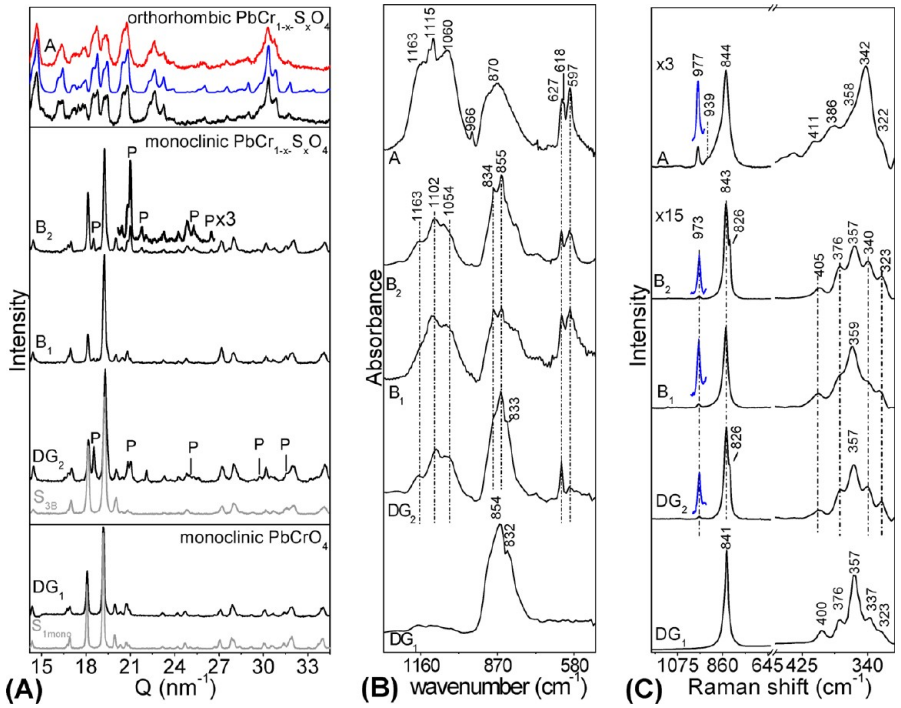

Figure 3. (A) XRD, (B) transmission mid-FTIR, and (C) Raman spectral data of the historic chrome yellow paints DG_1, DG_2, B_1, B_2, and A. In (A), the XRD pattern of sample A collected by the benchtop (black), portable (red), and SR-based (blue) device are shown. In gray, spectra of reference S_{1mono} and S_{3B}; P labels indicate the peaks of phoenicochroite.

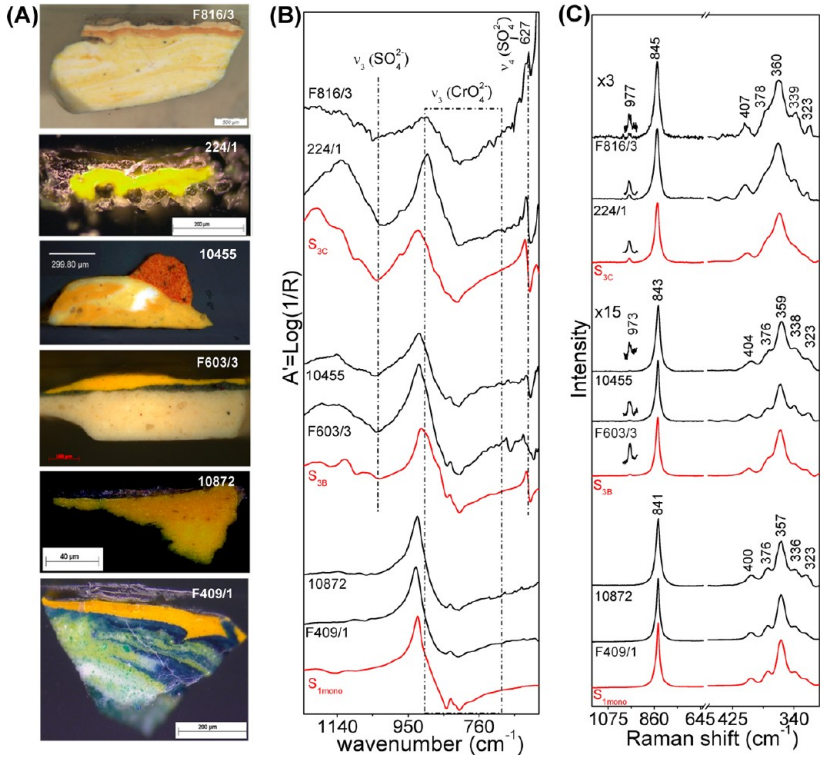

Figure 4. From top to bottom: (A) optical microscope images, (B) reflection mid-FTIR, and (C) Raman spectra collected from yellow areas of the original embedded paint microsamples F816/3, 224/1, 10455, F603/3, 10872, and F409/1 taken from different Van Gogh paintings (see Table 2 for further details). In (B) and (C), spectra of paints S_{1mono}, S_{3B}, and S_{3C} are illustrated in red color.

by the SR μ-XRD measurements (not shown in Figure 4, cf. Figure 1A). Although the μ-FTIR, Raman, and SR μ-XRD analyses clearly demonstrated only the presence of S-rich monoclinic $PbCr_{1-x}S_xO_4$ in F816/3 and 224/1, the additional presence of very low quantities of the orthorhombic phase cannot be excluded for these samples, since a coexistence of both monoclinic and orthorhombic $PbCr_{1-x}S_xO_4$ can be observed starting from an SO_4^{2-} molar amount of around 40%.[13]

dx.doi.org/10.1021/ac302158b | Anal. Chem. 2013, 85, 851−859

Finally, in order to ascertain whether or not it is possible to distinguish among different forms of $PbCr_{1-x}S_xO_4$ via non-invasive in situ measurements, we have examined Van Gogh's *Portrait of Gauguin* (Figure 5A) at the Van Gogh Museum using reflection mid-FTIR spectroscopy. The presence of bright yellow lacunae is visible on both the yellow and orange painted areas of the painting background. Figure 5A illustrates the locations in the yellow areas where FTIR spectra of Figure 5B were acquired. The resulting spectral data (four are shown as examples) show the presence of two inverted reststrahlen bands around 1039 cm^{-1} [$\nu_3(SO_4^{2-})$] and 822 cm^{-1} [$\nu_3(CrO_4^{2-})$], and two derivative-shape signals at 626 and 597 cm^{-1} [$\nu_4(SO_4^{2-})$]. These spectra show features in between those of the S_{3B} and S_{3C} model materials. The identification of a chrome yellow form, more similar to S_{3C}, is confirmed by Raman data obtained from a paint microsample (X448_2; Figure 5, panels A and C) from the painting itself. Likely due to the low abundance of the yellow pigment, no information about its presence was demonstrated by mid-FTIR analysis.

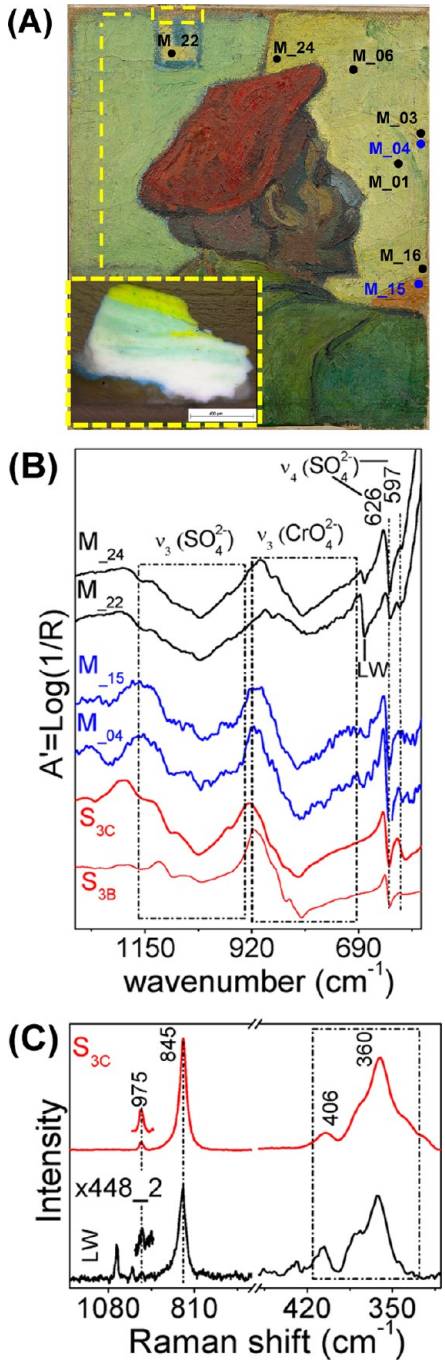

Figure 5. (A) Photographs of *Portrait of Gauguin* (37 × 33 cm, F546 s257v/1962) by Vincent van Gogh (1888, Van Gogh Museum, Amsterdam, The Netherlands) and a related microsample, X448_2. (B) Reflection mid-FTIR spectra recorded from the yellow lacunae (blue)and the outer pale yellow areas (black). (C) Raman spectrum (black) obtained from the yellow region of X448_2. In (A), labels indicate areas where FTIR data were acquired, while the dotted yellow rectangle points out the sampling location; LW shows the (B) bending and (C) stretching modes of CO_3^{2-} group of lead white. In (B and C) (red) spectra of paints S_{3B} and S_{3C}.

The identification of zinc white (inverted band at ca. 387 cm^{-1}, not shown in Figure 5B) and lead white (inverted band at ca. 1385 cm^{-1} and derivative signal at 687 cm^{-1}) in the outer yellow areas (M_22 and M_24), and that of barium sulfate (SO_4^{2-} combination bands,[27] not shown in Figure 5B) in the lacunae (M_04 and M_15) explains the subtle differences that are visible among the spectra of Figure 5B.

CONCLUSION

The combined use of analytical techniques such as XRD, FTIR, and Raman spectroscopy and SR-based methods such as SR μ-XRD and S K-edge μ-XANES permitted us to identify specific spectral features to distinguish among the different types of chrome yellow pigments in use at the end of the 19th century. The information acquired was used to investigate original chrome yellow samples taken from historic oil paint tubes and from paintings by Van Gogh and his contemporaries.

The study revealed that indeed different lead chromate-based pigments were used by these painters. The extended use by Van Gogh of monoclinic $PbCrO_4$, monoclinic $PbCr_{1-x}S_xO_4$, and mixtures of monoclinic and orthorhombic $PbCr_{1-x}S_xO_4$ was demonstrated. A co-precipitated $PbCr_{1-x}S_xO_4$ form was also found in one painting by Gauguin and in one sample from a palette used by Cézanne.

A relevant result is that the characterization of different chrome yellow forms is possible by using portable instrumentation. Preliminary in situ reflection mid-FTIR investigations performed on yellow areas of the painting, *Portrait of Gauguin* by Van Gogh, allowed us to identify the presence of $PbCr_{1-x}S_xO_4$ chrome yellow composed of a mixture of monoclinic and orthorhombic phases. This result was confirmed by laboratory measurements on a related microsample.

As described in the following paper (part 4),[18] the relation between the sulfate content, the crystal form, and the susceptibility to darkening during photochemical aging of different chrome yellow-based model paints has been investigated. The results demonstrate that the exact nature of the chrome yellow type strongly influences its long-term stability.

For this reason, future work will be dedicated to a detailed study by SR μ-XANES and μ-XRF investigations of a selection of the microsamples of Table 2, with the aim of exploring whether or not it is possible to establish an effective correlation between the chrome yellow composition/crystalline structure and the state of preservation of the pigment in original paintings. On the other hand, we will also seek to more systematically document the relation between the occurrence of the different types of chrome yellow and their exact hue/context/function in Van Gogh's work.

dx.doi.org/10.1021/ac302158b | *Anal. Chem.* 2013, 85, 851−859

■ ASSOCIATED CONTENT

Supporting Information

Additional information as noted in text. This material is available free of charge via the Internet at http://pubs.acs.org.

■ AUTHOR INFORMATION

Corresponding Author

*E-mail: koen.janssens@ua.ac.be. Tel: +32 3 265 33 22. Fax: +32 3 265 32 33.

Notes

The authors declare no competing financial interest.

■ ACKNOWLEDGMENTS

This research was supported by the Science for a Sustainable Development (SSD) Programme, Belgian Science Policy (S2-ART) and also presents results from GOA "XANES meets ELNES" (Research Fund University of Antwerp, Belgium) and FWO (Brussels, Belgium), Grants G.0704.08 and G.01769.09, respectively. The analysis of *Portrait of Gauguin* was performed within the MOLAB access activity of the EU FP7 programme CHARISMA (Grant 228330). MIUR (PRIN08, *Materiali e sistemi innovativi per la conservazione dell'arte contemporanea* 2008 FFXXN9), DESY/PETRA III (beamline P06), and ESRF (beamline ID21) are also acknowledged. Thanks are expressed to the staff of the Museé d'Orsay, the Van Gogh Museum, and the Kröller-Müller Museum for agreeable cooperation.

■ REFERENCES

(1) Hendriks, E. Van Gogh's Working Practice: A Technical Study. In *Vincent Van Gogh Paintings 2: Antwerp & Paris,1885−1888*; Hendriks, E., Van Tilborgh, L., Eds.; Waanders Publishers: The Netherlands, 2011; pp 90−143 and references therein.

(2) Bomford, D.; Kirby, J.; Leighton, J.; Roy, A. *Art in the Making: Impressionism*; National Gallery Publications: London, 1990; p 158.

(3) Monico, L.; Van der Snickt, G.; Janssens, K.; De Nolf, W.; Miliani, C.; Verbeeck, J.; Tian, H.; Tan, H.; Dik, J.; Radepont, M.; Cotte, M. *Anal. Chem.* **2011**, *83*, 1214−1223 and references therein.

(4) Monico, L.; Van der Snickt, G.; Janssens, K.; De Nolf, W.; Miliani, C.; Dik, J.; Radepont, M.; Hendriks, E.; Geldof, M.; Cotte, M. *Anal. Chem.* **2011**, *83*, 1224−1231 and references therein.

(5) Kühn, H.; Curran, M. Chrome Yellow and other Chromate Pigments. In *Artists' Pigments: A Handbook of Their History and Characteristics*; Feller, R. L., Ed.; Cambridge University Press: Cambridge, U.K., 1986: Vol. *1*, pp 187−200.

(6) Eastaugh, N.; Walsh, V.; Chaplin, T.; Siddall, R. *The Pigment Compendium* [CD-ROM]; Elsevier: Amsterdam, 2004.

(7) Jansen, L.; Luijten, H.; Bakker, N. *Vincent Van Gogh: The Letters*; Thames & Hudson Ltd.: London, 2009.

(8) Effenberger, H.; Pertlik, F. *Z. Kristallogr.* **1986**, *176*, 75−83.

(9) Korenberg, C. *British Museum Technical Research Bulletin* **2008**, *2*, 49−57.

(10) James, R. M.; Wood, W. A. *Proc. R. Soc. Lond., Ser. A* **1925**, *109*, 598−620.

(11) Cole, R. J. *The Research Association of British Paint, Colour and Varnish Manufacturers* **1955**, *10* (14), 1−62.

(12) Watson, V.; Clay, H. F. *J. Oil Colour Chem. Assoc.* **1955**, *38*, 167−177.

(13) Crane, M. J.; Leverett, P.; Shaddick, L. R.; Williams, P. A.; Kloprogge, J. T.; Frost, R. L. *Neues Jahrbuch für Mineralogie−Monatshefte* **2001**, *11*, 505−519.

(14) Colotti, G.; Conti, I.; Zocchi, M. *Acta Crystallogr.* **1959**, *12*, 416.

(15) Xiang, J.; Yu, S.; Xu, Z. *Cryst. Growth Des.* **2004**, *4*, 1311−1315.

(16) Otero, V.; Carlyle, L.; Vilarigues, M.; Melo, M. J. *RSC Adv.* **2012**, *2*, 1798−1805.

(17) Burnstock, A. R.; Jones, C. G.; Cressey, G. *Zeitschrift für Kunsttechnologie und Konservierung* **2003**, *17*, 74−84.

(18) Monico, L.; Janssens, K.; Miliani, C.; Van der Snickt, G.; Brunetti, B G.; Cestelli Guidi, M.; Radepont, M.; Cotte, M. *Anal. Chem.* **2012**, DOI: 10.1021/ac3021592.

(19) Rioux, J. P. *Dossier de l'art* **1999**, *55H*, 66−69.

(20) Miliani, C.; Rosi, F.; Brunetti, B. G.; Sgamellotti, A. *Acc. Chem. Res.* **2010**, *43*, 728−738.

(21) Cotte, M.; Susini, J.; Metrich, N.; Moscato, A.; Gratziu, C.; Bertagnini, A.; Pagano, M. *Anal. Chem.* **2006**, *78*, 7484−7492.

(22) Vairavamurthy, A. *Spectrochim. Acta, Part A* **1998**, *54*, 2009−2017.

(23) Figueiredo, M. O.; Pereira da Silva, T. *Eur. J. Mineral.* **2009**, *21*, 79−83.

(24) Alía, J. M.; Edwards, H. G. M.; Fernández, A.; Prieto, M. *J. Raman Spectrosc.* **1999**, *30*, 105−114.

(25) Doyen, L.; Frech, R. *J. Chem. Phys.* **1996**, *104*, 7847−7853.

(26) Stoilova, D.; Georgiev, M.; Marinova, D. *J. Mol. Struct.* **2005**, *738*, 211−215.

(27) Miliani, C.; Rosi, F.; Daveri, A.; Brunetti, B. G. *Appl. Phys. A: Mater. Sci. Process.* **2012**, *106*, 295−307.

(28) Wilkins, R. W. T. *Mineral. Mag.* **1971**, *38*, 249.

(29) Frost, R. L. *J. Raman Spectrosc.* **2004**, *35*, 153−158.